Ore Geology Reviews 145 (2022) 104876

Contents lists available at ScienceDirect

Ore Geology Reviews

journal homepage: www.elsevier.com/locate/oregeorev

Snowball Earth to global Warming: Coupled vanadium-carbonaceous deposits in the Cryogenian-Cambrian

John Parnell *

School of Geosciences, University of Aberdeen, Aberdeen AB24 3UE, United Kingdom

ARTICLE INFO

Keywords:
Vanadium
Green Energy
Critical elements
Black Shale
Graphite
Neoproterozoic
Cambrian

ABSTRACT

The anticipated high demand for new vanadium resources in support of the green energy revolution will be partly met by vanadium in carbonaceous deposits. This type of deposit is particularly developed during a 200 Myr period from Cryogenian-Cambrian. During this period, anoxic conditions were widely developed and provided a template for vanadium deposition. Vanadium became available to the surface during the Neoproterozoic when anomalously high levels were introduced in large igneous provinces. Global glacial erosion transported vanadium to the oceans, along with trace elements that engendered organic carbon accumulation. The combination of vanadium and organic carbon gave rise to a range of deposits, and provides a model to support exploration for further resources.

1. Introduction

Green energy requires a step change in the use of minerals. For example, wind energy technology needs a much greater mineral resource than fossil fuel-based technology (International Energy Agency 2022). Battery performance is widely highlighted as a driver for metal and graphite exploration. The vanadium-flow battery is an option to help address the needs of the green energy revolution (Parasuraman et al. 2013, Zhang et al. 2019, Gencten & Sahin 2020). The manufacture of the batteries will require additional resources of vanadium, and hence prompted new exploration and mining projects in many countries (Colthorpe 2021). One of the most promising deposits is the Green Giant vanadium deposit in Madagascar (Scherba et al. 2018). The vanadium deposit is spatially associated with graphite deposits, both of which are licenced by a single exploration company. The association is widely described as serendipitous (Nextsource Materials 2017). However, a review of vanadium deposits in shale sequences shows that the association of vanadium with carbon-rich sediments was well developed in Cryogenian-Cambrian successions, i.e. ~ 700–500 Ma (Fig. 1; Table 1). The widespread occurrence of this association, which had not been evident in the earlier geological record, suggests that the availability of vanadium had markedly increased.

2. The anomalous supply of vanadium

The abundance of vanadium at the Earth's surface rose distinctly during the Neoproterozoic. Several data sets reflect the trend (Fig. 2). Firstly, the number of distinct vanadium minerals increased sharply (Moore et al. 2020), reflecting both the number of localities where they are recorded and the formation of alteration products following atmospheric oxygenation. Secondly, the V content of marine pyrite increased as the concentration increased in sea water (Mukherjee & Large 2020). Thirdly, the maximum V content of black shales increased, also reflecting sea water composition (Sahoo et al. 2012).

Enrichment of the Neoproterozoic crust in vanadium was heralded by global magmatic activity (Li et al. 2008). Vanadium V^{3+} ions have an ionic radius similar to Fe^{3+} ions, so V commonly substitutes for Fe in magnetite and ferromagnesian silicate minerals formed during magmatism. Consequently, mafic rocks are relatively enriched in V. Following Neoproterozoic magmatism, global Sturtian glaciation at ~ 700 Ma, and younger Neoproterozoic glaciations, enhanced V availability. Glacial erosion contributes much finely ground material into the oceans (Anderson 2007), and the glacial events especially caused extensive deep erosion of vanadium-enriched crust, bringing vanadium to the surface environment just as increasing oxygen levels contributed to its mobility.

An anomalous vanadium enrichment in the magmatic rocks is evident in the detailed chemistry of Neoproterozoic igneous provinces.

* Corresponding author.
E-mail address: J.Parnell@abdn.ac.uk.

https://doi.org/10.1016/j.oregeorev.2022.104876
Received 7 December 2021; Received in revised form 28 March 2022; Accepted 6 April 2022
Available online 9 April 2022

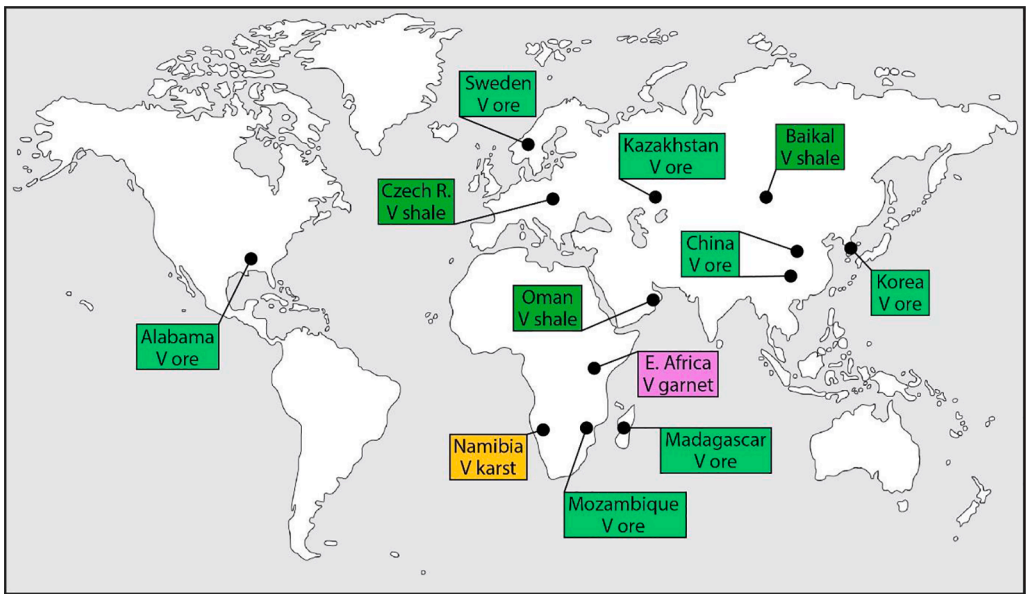

Fig. 1. Global map, showing occurrences of vanadium ore, and other vanadium concentrations in carbonaceous sediments of Cryogenian-Cambrian age.

A review of three igneous provinces in which glacial erosion excavated the volcanic rocks and incorporated them into the glacial deposits consistently shows compositions several times the upper continental crust average of 60 ppm V and higher than the basalt average of 250 ppm V (Kelley et al. 2017). The high V contents are also shown by igneous provinces at the end of the Neoproterozoic, which post-dated the glaciations but were eroded into the Cambrian oceans.

Weathering of the Neoproterozoic basalts has been implicated in the drawdown of carbon dioxide and cooling, which prompted the Sturtian glaciation (Lenton et al. 2014, Goddéris et al. 2003, Cox et al. 2016, Donnadieu et al. 2004). The basalts of this magmatic episode would have been highly weatherable (Goddéris et al. 2003, Lenton et al. 2014), and the weathering of an atypically large volume of basalt at that time would have liberated anomalous amounts of vanadium to surface systems. The average basalt has a vanadium content about twelve times that of the average granite (mean values 250 ppm basalt, 20 ppm granite) (Kelley et al. 2017), which would normally have dominated the detritus from eroding continents. Considering the greater susceptibility of basalt to weathering, up to twenty times faster than granitic rocks (Horton 2015), the erosion of typical basaltic terrain might increase the flux of vanadium by two orders of magnitude relative to typical granitic terrain. The contrast would have been even greater in the Neoproterozoic, when basalts contain vanadium levels higher than the average basalt. The model for accelerated weathering is based on basalts on the Laurentian continent (Mills et al. 2014, Donnadieu et al. 2004, Horton 2015), where the Franklin Igneous Province (FIP) covers an area exceeding 2 million km^2. A direct contribution from FIP basalts is evident in Alaska where they interfinger with glacial diamictite and contribute clasts to it (Macdonald 2011). Several data sets from Alaska to Greenland show mean vanadium levels in the FIP nearly 50% greater than those of average basalts (Fig. 3, Table 2). The weighted mean of the data sets is 351 ppm V (n = 167). These statistics combine to indicate the liberation of vanadium by weathering of the FIP up to 350 times that of granitic terrain, independent of any additional enhancement due to rapid glacial weathering.

The FIP was not the only large igneous province whose rocks were sequestered by Sturtian glaciation (Fig. 4). Neoproterozoic basalts in Australia, including volcanics in the Gairdner Igneous Province, are also V-rich. Seven data sets for basalts all have mean contents well above the mean basalt composition of 250 ppm V, and a weighted mean value of 346 ppm V (n = 61) (Table 2). There is direct evidence for the erosive downcutting of glacial beds into the basalts by the Sturtian glaciation, and the resultant incorporation of basalt clasts in the tillite (Mitchell et al. 2019). Similarly, four data sets for basalts in the Anti-Atlas Supergroup in Morocco have mean contents above 300 ppm V, and a weighted mean value of 321 ppm V (n = 46) (Table 2). Glacial diamictites there have incorporated volcanic clasts (Letsch et al. 2018). Furthermore, neodymium isotope data indicate an enhanced contribution of eroded magmatic rock to marine sediments from about 750 to 600 Ma (Horton 2015), confirmingthat the potential of this volcanic feedstock was realized.

The high availability of vanadium continued after the glaciations, including for example basalts of the Dalradian Supergroup in Britain and Ireland, and flood basalts of the Volyn Large Igneous Province across Eastern Europe, Belarus and Ukraine. They have weighted mean values of 376 ppm V (n = 43) and 369 ppm V (n = 45) respectively. The continuing supply of vanadium, in the latter part of the Neoproterozoic, was available to surface environments in the Lower Palaeozoic, especially the Cambrian.

Following the delivery of abundant V to the upper crust, availability of the V was facilitated by the higher oxygen content of the atmosphere from the late Neoproterozoic onwards. Increased oxygen allowed greater concentrations of dissolved V in surface waters and seawater (Moore et al. 2020). Prior to the late Neoproterozoic, when oceans were anoxic, levels of dissolved V were relatively low. Then in the late Neoproterozoic V was readily available for incorporation into anoxic sediments.

The combination of repeated mafic volcanism, global glacial erosion, and oxygenation of the atmosphere set the scene for vanadium enrichment of anoxic sea floor sediments.

Table 1
Vanadium deposits associated with carbonaceous rocks within Cryogenian-Cambrian time.

Country	Major vanadium deposit	Formation	Age (Ma)	Organic carbon	V_2O_5 resource	Exploration Company	Reference
Madagascar	Green Giant	Tolagnaro-Ampanihy Complex, Graphite Beds	800–580	Ore up to >10 % TOC (mined)	60 Mt V_2O_5 (cut-off 0.5 %)	Nextsource Materials Inc.	Scherba et al. 2018
Mozambique	Balama	Xixano Complex	800–600	Ore up to 17.5 % TOC (mined)	1.422 Bt at 0.2 % V_2O_5	Syrah Resources	Dickinson 2015
Mozambique	Nicanda Hill	Xixano Complex	800–600	Ore mean 10.7 % TOC (mined)	3.93 Mt V_2O_5	Triton Minerals	Dickinson 2014
Mozambique	Caula	Xixano Complex	800–600	Up to 29 % TOC (mined)	82 Kt V_2O_5	New Energy Minerals	New Energy Minerals 2019
East Antarctica		Steingarden nunataks	720–630	25–30 vol% graphite	Rich in vanadian micas	(not commercial)	Schlüter et al. 2011
Tanzania-Kenya	Tsavorite gem deposits	Mozambique Belt	720 Met. at ~ 600	16 % TOC (mined at Chenjere)	Vanadian garnet gems	(gem collection)	Giuliani et al. 2018
Baikal, Russia		Olkhon & Sludyanka complexes	670–500	Up to 10 % TOC (once mined)	Up to 1785 ppm V_2O_5	(not commercial)	Koneva 1997
Namibia	Abenab	Otavi Gp.	635–535 (Tertiary mobilization)	Up to 9 % TOC	1.85 Mt ore at 1.03 % V_2O_5	Broadway Gold Mining	Kamona & Günzel 2007
Korea	Daejon	Changri Fm.	600–500	Up to 57 % TOC (mined as coal)	248 Mlbs 2000 + ppm V (Daejon deposit)	Optiro	Jeong 2006
China	Baiguoyuan	Doushantuo Fm.	600–540	Up to 4.9 % TOC (shale gas potential)	1 Bt ore in Chinese Ediacaran, at 3.24 % V_2O_5	Huili Resources	Zhuang et al. 1998
Czech Republic		Blovice Complex	560–535	Up to 4.9 % TOC	Up to 3600 ppm V_2O_5	(not commercial)	Kurzweil et al. 2015
Alabama, USA	Coosa	Ediacaran-Cambrian Higgins Ferry Gp.	540	Graphite (mined)	Up to 4000 ppm V_2O_5	Westwater Resources	Dean 2002
Oman		Ediacaran-Cambrian boundary	540	Up to 9 % TOC	Up to 5000 ppm V_2O_5	(not commercial)	Schröder & Grotzinger 2007
Kazakhstan	Karatau	Lower Cambrian	530	8–10 % TOC (resource)	2.01 Mt ore Av. 1.0%	Balausa	Dzhumankulova et al. 2020
China	Yangjiabu and others	Lower Cambrian 'stone coal'	530	15 to 25 % TOC on average (mined as coal)	118 Mt V_2O_5 (Zhang et al. 2011) 55.3 Bt ore at 0.13 to 1.2 % V_2O_5 (Dai et al. 2018)	Rentian Mining Ltd. Tengda Mining Ltd.	Zhang et al. 2011,Dai et al. 2018
United Kingdom		Upper Cambrian White-leaved Oak Shale	500	Up to 5 % TOC	Up to 4000 ppm V_2O_5	(not commercial)	Author's unpublished data
Sweden	Häggån	Upper Cambrian Alum Shale	495	Up to 20 % TOC (regionally mined for oil)	2 Bt ore at 0.3 % V_2O_5	Aura Energy	Bian et al. 2021

TOC: Total Organic Carbon.

3. Vanadium in carbon-rich sediments in the Cryogenian-Cambrian

Carbon-rich sediments were deposited following the late Neoproterozoic 'Snowball Earth' glaciations, when the oceans were flooded with fresh nutrients which supported extensive microbial growth (Planavsky et al. 2010). The development of anoxia, promoting the preservation of organic carbon, continued through the Cambrian, most notably in the Upper Cambrian Alum Shale in Europe. This period of about 200 million years saw the biggest peak in black shale sedimentation over the last 1500 million years (Condie et al. 2001).

Under anoxic conditions, V was incorporated in carbon-rich sediments as silicates and associated with organic matter (Breit & Wanty 1991). As carbonaceous rocks are metamorphosed, their clay minerals are converted to micas, which helps the sequestration of V. The main residence of V in (meta-)sedimentary rocks is in vanadian mica (Fig. 5), often the mineral roscoelite. Accordingly, graphitic rocks containing V are commonly characterized by green micas, i.e. roscoelite. The record of V deposits in carbon-rich sediments through Cryogenian-Cambrian time shows a range from organic- and clay-hosted V (e.g. Alum Shale; Lerat et al. 2018) to roscoelite-hosted V (e.g. Mozambique), related to the degree of metamorphism. Exceptionally, continued metamorphism in a sequence that also contains *meta*-evaporites caused expulsion of V from sheet silicates to form vanadian garnets (tsavorite) in East Africa (Feneyrol et al. 2013, Giuliani et al. 2018). Tsavorite deposits occur in Neoproterozoic graphitic gneisses in Madagascar, Tanzania and Kenya, accompanied by V-rutile, V-kyanite, V-muscovite, V-zoisite and V-pyrrhotite (Giuliani et al. 2018) and Antarctica (Osanai et al. 1990). The tsavorite deposits are not a commercial source of V, but serve to emphasize the strong link between V accumulation and carbon-rich sediments during Cryogenian-Cambrian time. In a further variation in south west Africa, especially Namibia, V-bearing Neoproterozoic rocks were extensively weathered to leave V-mineralized karst during the Paleogene, including what were once among the richest V deposits in the

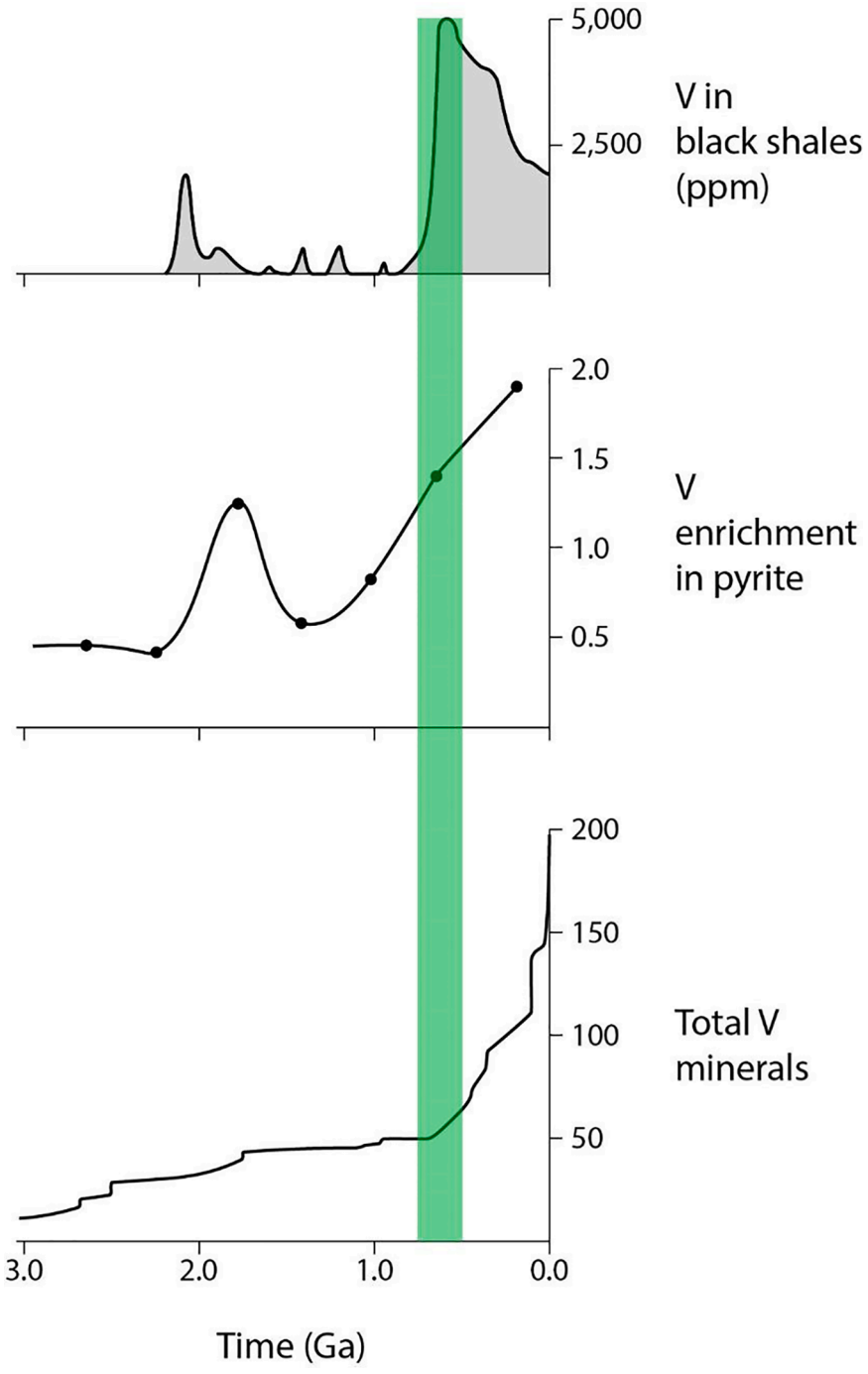

Fig. 2. Increase in V abundance in Neoproterozoic, recorded by (i) maximum V content in black shales (Sahoo et al. 2012), (ii) V content in marine pyrite, expressed as ratio to long-term mean content (Mukherjee & Large 2020), and (iii) number of V minerals (Moore et al. 2020).

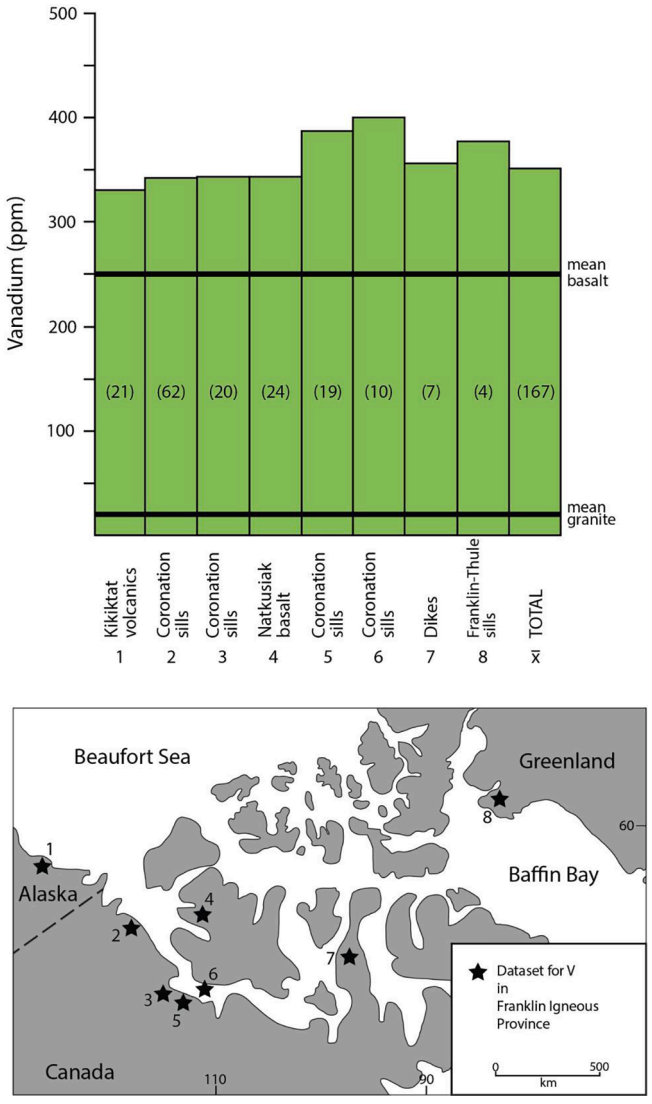

Fig. 3. Anomalous vanadium contents in Franklin Igneous Province. Vanadium contents shown for 8 sets of samples, and mean value, relative to global mean values for basalt and granite. Data sources in Table 2.

world (Kamona & Günzel 2007).

The result of V incorporation in carbon-rich sediments gave rise to a range of actual and potential V deposits (Table 1), and also anomalously V-rich sediments that are unlikely to be commercial. Those deposits that are commercial have estimated tonnages, although these cannot be fully compared as they are calculated using different cut-off values. This review adopts a cut-off of 500 ppm V to identify anomalously high content, as also made by Kunert et al. (2020) and some commercial resource evaluations. In each case the sediment is also exceptionally rich in carbon, which in several instances is/was mined as graphite, or is exploitable as an alternative carbonaceous product such as oil or shale gas. The association of exceptional carbon and exceptional V implies that the V content scales with the carbon content. This means that a typical back shale with a few % TOC, rather than an exceptionally rich black shale (richer than an excellent oil source rock with 3 % TOC) may have a V content that is moderately rich but not commercially viable. For example, Cryogenian shales at Bluefish Creek, north west Canada, with up to 1.85 % TOC, have a mean 233 ppm V (Sperling et al. 2016). Unlike many metals, V does not form discrete sulphides, or trace substitutions in pyrite, during diagenesis (Kunert et al. 2020), and consequently V is not richer in pyritic shales.

The Cryogenian-Cambrian record of the vanadium-carbon association includes three particular stages that are distributed over a large area. The oldest is the Neoproterozoic Mozambique Belt in East Africa (broadly dated at 800–600 Ma), particularly in Madagascar and Mozambique. There are Lower Cambrian deposits across much of southern China, and possibly related deposits in adjacent Korea, Kazakhstan and the Baikal region of Siberia. In Europe, deposits are dominated by the Upper Cambrian Alum Shale, and the immediately following (Tremadoc = basal Ordovician) Dictyonema Shale, in Sweden and the Baltic States.

4. Discussion

4.1. Transfer of vanadium from volcanic rocks

The data show that Neoproterozoic igneous provinces provided a high mass of vanadium to the surface, and that on the Neoproterozoic sea floor anoxic sediments incorporated a high mass of vanadium. In addition to the systematic processes of weathering, erosion and transport that link the two together, the mid-Neoproterozoic witnessed the exceptional imprint of at least two global glaciations, the first of which lasted for tens of millions of years. The huge scale at which Neoproterozoic glacial erosion transferred mass from continent to ocean is evident from a local thickness of glacial debris exceeding 3 km (Young & Gostin 1989), denudation of at least 6 km in North America over 850–680 Ma deduced by thermochronology (DeLucia et al. 2018) and an estimated global erosion through 3–5 km due to glaciation (Keller et al. 2019). The Neoproterozoic glacial erosion has been invoked to explain the delivery of anomalous quantities of phosphorus (Horton 2015), copper (Parnell & Boyce 2019), and nutrients in general (Planavsky et al. 2010) to the oceans, and the evidence indicates that anomalous V was similarly delivered.

4.2. Stratigraphic record of vanadium deposits

The abundance of V deposits in Cryogenian-Cambrian carbon-rich rocks reflects the peak in black shale sedimentation identified by Condie et al. (2001). Within that interval, rocks deposited under anoxic conditions are represented particularly by the Neoproterozoic Mozambique Belt in East Africa, Lower Cambrian deposits across much of China, and the Upper Cambrian Alum Shale and equivalents in northern Europe. The distribution of V deposits maps onto this distribution of anoxic sediments. Notably, these three sub-episodes are in different parts of the globe (and were also during the Cambrian), implying that the source of V was in globally distributed ocean water rather than a discrete source.

4.3. Consequences for vanadium exploration

The biggest peak in black shale sedimentation in Earth's history was in the Palaeoproterozoic (~2.0 Ga). However, although there are many other types of ore deposits related to these rocks (Parnell et al. 2021), there is little recorded concentration of vanadium. This implies that the abundance of carbon was not the sole factor behind V accumulation. The data from igneous provinces shows that there was a readily available source of V in the Neoproterozoic, which was newly mobile as the atmosphere became oxygenated. Exploration in carbon-rich sediment is therefore best focussed on the Neoproterozoic and younger successions.

Future exploration is most likely to be successful in extensions to the three large belts in the Neoproterozoic of East Africa, Lower Cambrian of China, and the Upper Cambrian in northern Europe. In East Africa, there are discoveries of graphite in Ethiopia, Sudan and Egypt in the northern equivalent of the Mozambique Belt, where exploration for trace elements including vanadium could be undertaken (Asia Pacific Gold Mining Investment Ltd. 2013). The Lower Cambrian deposits in China are widespread, and exploration benefits from historical artisanal mining of stone coal as a domestic fuel. A range of technologies are being assessed to release the vanadium from the stone coal matrix (Peng 2019,

Table 2
Vanadium contents in volcanic rocks in Neoproterozoic igneous provinces.

Igneous Province	Locality	Stratigraphy	Number analyses	Mean V (ppm)	Reference
Franklin	Alaska	Kikiktat Volcanics	21	330	Cox et al. 2015
Franklin	Brock	Coronation sills	62	342	Bédard et al. 2016
Franklin	Coppermine	Coronation sills	20	343	Bédard et al. 2016
Franklin	Victoria Island	Natkusiak Basalt	24	343	Williamson et al. 2016
Franklin	Coronation Gulf	Coronation sills	19	387	Shellnutt et al. 2004
Franklin	Murray Island	Coronation sills	10	400	Bédard et al. 2016
Franklin	Somerset, POW islands	Dikes	7	356	Bédard et al. 2016
Franklin	NW Greenland	Franklin-Thule sills	4	377	Kettanah et al. 2016
		Weighted mean	**167**	**351**	
Gairdner	Stuart Shelf	Bitter Springs Volcanics	3	337	Zhao et al. 1994
Gairdner	Adelaide Fold Belt	Wooltana Volcanics	7	351	Foden et al. 2002
Gairdner	Adelaide Fold Belt	Wooltana Volcanics	14	320	Wang et al. 2010
Gairdner	Stuart Shelf	Beda Basalt	9	357	Wade et al. 2014
Gairdner	Amadeus Basin	Amata Suite	4	377	Zhao et al. 1994
Gairdner	Adelaide Fold Belt	Deport Creek Volcanics	6	366	Wang et al. 2010
Gairdner	Officer Basin	Keene Basalt	18	346	Zi et al. 2019
		Weighted mean	**61**	**346**	
Anti-Atlas Supergroup	Morocco	Ait Ahmane-Khzama Ophiolite	10	310	Hodel et al. 2020
Anti-Atlas Supergroup	Morocco	Bleida-Tachdamt Gp. II/IV	7	373	Leblanc & Moussine-Pouchkine 1994
Anti-Atlas Supergroup	Morocco	Siroua Massif	7	351	Boukhari et al. 1992
Anti-Atlas Supergroup	Morocco	Bou Azzer Ophiolite	22	300	Naidoo et al. 1991
		Weighted mean	**46**	**321**	
Dalradian Supergroup	Scotland, U.K.	Easdale Subgroup basalts	23	381	Fettes et al. 2011
Dalradian Supergroup	Scotland, U.K.	Muckle Fergie Burn basalt	1	344	Chew et al. 2010
Dalradian Supergroup	Scotland, U.K.	Perthshire dolerite sills	7	379	Graham & Bradbury 1981
Dalradian Supergroup	Scotland, U.K.	Farragon Beds	12	367	Goodman & Winchester 1993
		Weighted mean	**43**	**376**	
Volyn-Brest	Ukraine	Volyn Series	7	388	Kuzmenkova et al. 2011
Volyn-Brest	Ukraine	Volyn Series	5	353	Białowolska et al. 2002
Volyn-Brest	Belarus-Ukraine	Volyn Series	17	361	Nosova et al. 2008
Volyn-Brest	Moldova-Belarus-Ukraine	Volyn Series	16	397	Środoń et al. 2019
		Weighted mean	**45**	**369**	

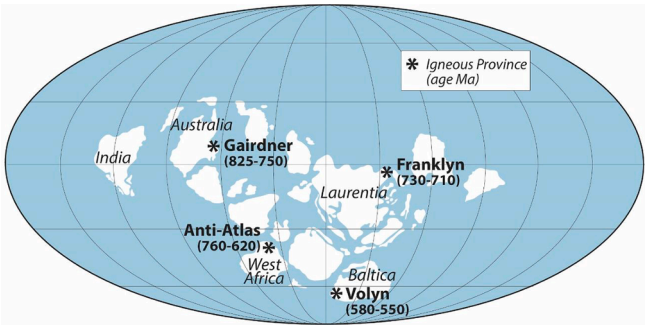

Fig. 4. Global palaeogeography at 630 Ma (after Li et al. 2008), showing location of Neoproterozoic igneous provinces (Gairdner, Franklin, Anti-Atlas, Volyn) with V-rich basalts.

Fig. 5. Graphitic schist containing V-rich micas, Neoproterozoic, Dronning Maud Land, East Antarctica (image courtesy of Jochen Schlüter, Cornelia Spiegel and colleagues, Hamburg and Bremen).

Wang et al. 2020). The extraction of vanadium from stone coal would be done in combination with the extraction of other elements including rare earth elements and platinum group elements (Dai et al. 2018, Wu et al. 2021). The Lower Cambrian Karatau deposit in Kazakhstan could similarly be co-exploited for other metals (Kenzhaliyev et al. 2021). Vanadium exploration in the Upper Cambrian in Europe is currently problematic because of environmental considerations, although several potential sites in Sweden have been identified (Tellerreport 2019). However, this potential may yet be realised, as geopolitical considerations become more urgent. Not only is much of the world's vanadium produced in China, but many deposits in other countries are financed by, and destined for, China (Barrera 2020).

Where both resources are co-located (Fig. 6), the co-exploration of vanadium and carbon (graphite) has obvious advantages in terms of shared infrastructure and other costs. This is especially relevant in East Africa where companies can licence for both vanadium and graphite (Syrah Resources Ltd. 2021). The association is regarded as fortuitous, but the evidence of this review is that it is not. As both commodities are required for future batteries, they can be cast as jointly contributing to the needs of green energy technology. While vanadium in East Africa is associated with resources of graphite, the Cambrian deposits in China are associated with less ordered carbon, which is used as a fuel in power stations and the domestic market (Dai et al. 2018).

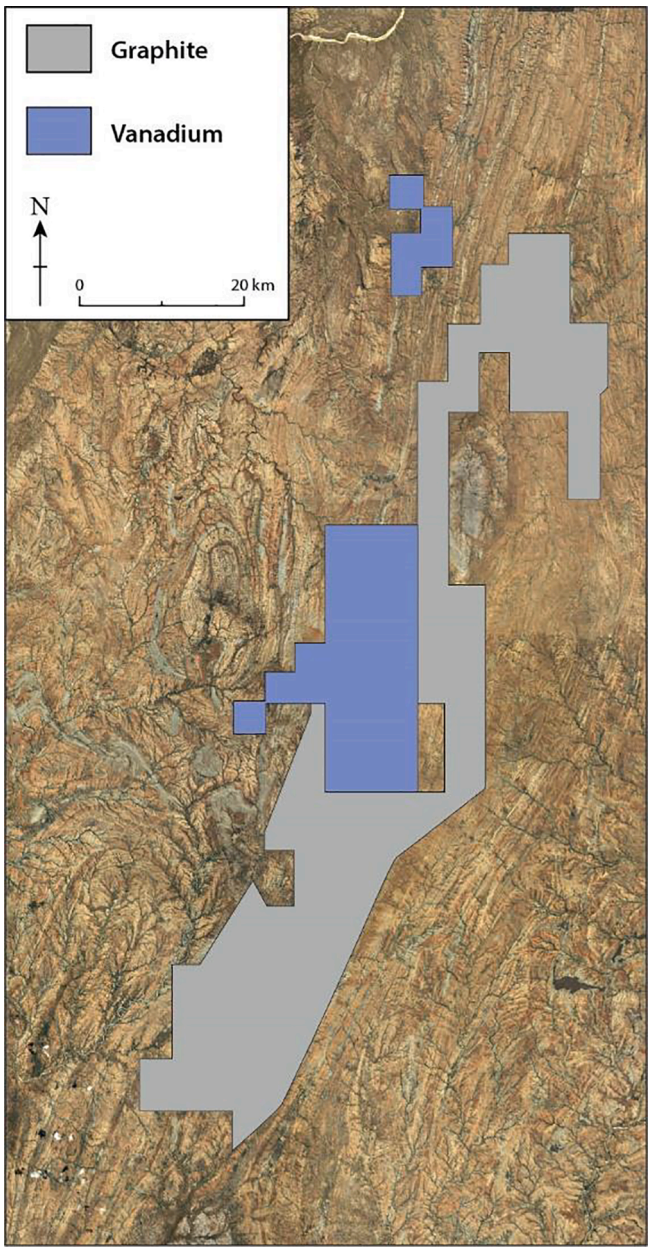

Fig. 6. Licence map for exploration for graphite and vanadium, Green Giant property, Madagascar. Licenced ground is contiguous, allowing efficient co-exploration.

5. Conclusions

Vanadium deposits related to carbon-rich sediments were formed particularly during Cryogenian-Cambrian time. The association reflects the availability of large amounts of vanadium in igneous provinces, the transfer of the vanadium into the oceans enhanced by global glacial erosion, and the deposition of anomalously carbon-rich sediments in which the vanadium accumulated.

The association is yielding vanadium in several parts of the world, and several more are at the exploration/development stage. There is good knowledge of where the carbonaceous host rocks are, including graphite deposits, which should focus the exploration for vanadium. With better understanding of how the association was developed in Cryogenian-Cambrian time, further vanadium resources can be expected.

Declaration of Competing Interest

The authors declare that they have no known competing financial interests or personal relationships that could have appeared to influence the work reported in this paper.

Acknowledgements

I am grateful to J.Johnston and J. Bowie for skilled technical support. The research was partly supported by NERC grant NE/T003677/1. The manuscript benefitted from the comments of two reviewers.

References

Anderson, S.P., 2007. Biogeochemistry of glacial landscape systems. Annual Review of Earth and Planetary Sciences 35, 375–399.

Asia Pacific Gold Mining Investment Ltd. 2013. Asia Pacific Gold Mining Investment Ltd announces graphite potential in western Ethiopia. https://www.investegate.co.uk/asia-pacific-gold-mining-inves–apgm-/prn/announces-graphite-potential-in-western-ethiopia/20130930095355PB1D8/.

Barrera, P. 2020. Vanadium Outlook 2021: Strong Chinese demand expected, but uncertainty remains. Vanadium Investing News, December 30, 2020. https://investingnews.com/daily/resource-investing/battery-metals-investing/vanadium-investing/vanadium-outlook/.

Bédard, J.H., et al., 2016. Geochemical database of Franklin sills, Natkusiak Basalts and Shaler Supergroup rocks, Victoria Island, Northwest Territories, and correlatives from Nunavut and the mainland. Geological Survey of Canada, Open File 8009, 1.zip file. https://doi.org/10.4095/297842.

Białowolska, A., Bakun-Czubarow, N., Fedoryshyn, Y., 2002. Neoproterozoic flood basalts of the upper beds of the Volhynian Series (East European Craton). Geological Quarterly 46, 37–57.

Bian, L., Schovsbo, N.H., Chappaz, A., Zheng, X., Nielsen, A.T., Ulrich, T., Wang, X., Dai, S., Galloway, J.M., Małachowska, A., Xu, X., Sanei, H., 2021. Molybdenum-uranium-vanadium geochemistry in the Lower Paleozoic Alum Shale of Scandinavia: Implications for vanadium exploration. International Journal of Coal Geology 239 (2021), 103730.

Boukhari, A.E., Chabane, A., Rocci, G., Tane, J., 1992. Upper Proterozoic ophiolites of the Siroua Massif (Anti-Atlas, Morocco) a marginal sea and transform fault system. Journal of African Earth Sciences 14, 67–80.

Breit, G.N., Wanty, R.B., 1991. Vanadium accumulation in carbonaceous rocks: A review of geochemical controls during deposition and diagenesis. Chemical Geology 91, 83–97.

Chew, D.M., Fallon, N., Kennelly, C., Crowley, Q., Pointon, M., 2010. Basic volcanism contemporaneous with the Sturtian glacial episode in NE Scotland. Transactions of the Royal Society of Edinburgh: Earth Sciences 100, 399–415.

Colthorpe, A. 2021. Growing interest from battery sector is driving vanadium demand growth. https://www.energy-storage.news/news/growing-interest-from-battery-sector-is-driving-vanadium-demand-growth.

Condie, K.C., Des Marais, D.J., Abbott, D., 2001. Precambrian superplumes and supercontinents: a record in black shales, carbon isotopes, and paleoclimates? Precambrian Research 106, 239–260.

Cox, G.M., et al., 2015. Kikiktat volcanics of Arctic Alaska – Melting of harzburgitic mantle associated with the Franklin large igneous province. Lithosphere 7, 275–295.

Cox, G.M., et al., 2016. Continental flood basalt weathering as a trigger for Neoproterozoic Snowball Earth. Earth and Planetary Science Letters 446, 89–99.

Dai, S., Zheng, X., Wang, X., Finkelman, R.B., Jiang, Y., Ren, D., Yan, X., Zhou, Y., 2018. Stone coal in China: a review. International Geology Review 60, 736–753.

Dean, L.S., 2002. Minerals in the Economy of Alabama. In: Fousek, R.S. (Ed.), The Geology. Alabama Geological Society, Mining Methods and Processing of Selected Industrial Minerals in Northeastern Alabama, pp. 1–26.

DeLucia, M.S., Guenthner, W.R., Marshak, S., Thomson, S.N., Ault, A.K., 2018. Thermochronology links denudation of the Great Unconformity surface to the supercontinent cycle and snowball Earth. Geology 46, 167–170.

Dickinson, R., 2014. Triton's Nicanda Hill show rolls on. Australia's Paydirt 1 (221), 51.

Dickinson, R., 2015. Metals of Africa resurrects Balama Central. Australia's Paydirt 1 (232), 55.

Donnadieu, Y., Goddéris, Y., Ramstein, G., Nédélec, A., Meert, J., 2004. A 'snowball Earth' climate triggered by continental break-up through changes in runoff. Nature 428, 303–306.

Dzhumankulova, S.K., Zhuchkov, V.I., Alybaev, Z.A., Bekenova, G.K., 2020. Review of state and prospects for development of vanadium production in the Kazakhstan Republic. Metallurgist 64, 75–81.

Feneyrol, J., et al., 2013. Worldwide tsavorite deposits: new aspects and perspectives. Ore Geology Reviews 5, 1–25.

Fettes, D.J., Macdonald, R., Fitton, J.G., Stephenson, D., Cooper, M.R., 2011. Geochemical evolution of Dalradian metavolcanics rocks: implications for the break-up of the Rodinia supercontinent. Journal of the Geological Society, London 168, 1133–1146.

Foden, J., Song, S.H., Turner, S., Elburg, M., Smith, P.B., Van der Steldt, B., Van Penglis, D., 2002. Geochemical evolution of lithospheric mantle beneath S.E. South Australia. Chemical Geology 182, 663–695.

Gencten, M., Sahin, Y., 2020. A critical review on progress of the electrode materials of vanadium redox flow battery. International Journal of Energy Research 44, 7903–7923.
Giuliani, G., et al., 2018. The role of evaporites in the formation of gems during metamorphism of carbonate platforms: a review. Mineralium Deposita 53, 1–20.
Goddéris, Y., et al., 2003. The Sturtian 'snowball' glaciation: fire and ice. Earth and Planetary Science Letters 211, 1–12.
Goodman, S., Winchester, J.A., 1993. Geochemical variations within metavolcanic rocks of the Dalradian Farragon Beds and adjacent formations. Scottish Journal of Geology 29, 131–141.
Graham, C.M., Bradbury, H.J., 1981. Cambrian and late Precambrian basaltic igneous activity in the Scottish Dalradian: a review. Geological Magazine 118, 27–37.
Hodel, F., Triantafyllou, A., Berger, J., Macouin, M., Baele, J.-M., Mattielli, N., Monnier, C., Trindade, R.I.F., Ducea, M.N., Chatir, A., Ennih, N., Langlade, J., Poujol, M., 2020. The Moroccan Anti-Atlas ophiolites: Timing and melting processes in an intra-oceanic arc-back-arc environment. Gondwana Research 86, 182–202.
Horton, F., 2015. Did phosphorus derived from the weathering of large igneous provinces fertilize the Neoproterozoic ocean? Geochemistry, Geophysics, Geosystems 16, 1723–1738.
International Energy Agency, 2022. The Role of Critical Minerals in Clean Energy Transitions. International Energy Agency, Paris https://www.iea.org/reports/the-role-of-critical-minerals-in-clean-energy-transitions.
Jeong, G.Y., 2006. Mineralogy and geochemistry of metalliferous black slates in the Okcheon metamorphic belt, Korea: a metamorphic analogue of black shales in the South China block. Mineralium Deposita 41 (5), 469–481.
Kamona, A.F., Günzel, A., 2007. Stratigraphy and base metal mineralization in the Otavi Mountain Land, Northern Namibia – a review and regional interpretation. Gondwana Research 11, 396–413.
Keller, C.B., et al., 2019. Neoproterozoic glacial origin of the Great Unconformity. Proceedings of the National Academy of Sciences 116, 1136–1145.
Kelley, K.D., Scott, C.T., Polyak, D.E., and Kimball, B.E., 2017, Vanadium, chapter U of Schulz, K.J., DeYoung, J.H., Jr., Seal, R.R., II, and Bradley, D.C., eds., Critical mineral resources of the United States—Economic and environmental geology and prospects for future supply: U.S. Geological Survey Professional Paper 1802, p. U1–U36, https://doi.org/10.3133/pp1802U.
Kenzhaliyev, B.K., Surkova, Yu., Azlan, M.N., Yulusov, S.B., Sukurova, B.M., Yessimova, D.M., 2021. Black shale ore of Big Karatau is a raw material source of rare and rare earth elements. Hydrometallurgy 205, 105733.
Kettanah, Y., Zentilli, M., Hanley, J., Tweedale, F., 2016. Geological setting and fluid inclusion characteristics of a lead-copper-barium occurrence hosted in a Neoproterozoic mafic sill at Kiatak, Northumberland Island, Northwestern Greenland. Ore Geology Reviews 79, 268–287.
Koneva, A.A., 1997. Cr-V-manganospinels in metamorphic rocks, Lake Baikal, Russia. Mineralogical Magazine 61, 145–148.
Kunert, A., Clarke, J., Kendall, B., 2020. Molybdenum isotope constraints on the origin of vanadium hyper-enrichments in Ediacaran-Phanerozoic marine mudrocks. Minerals 10, 1075. https://doi.org/10.3390/min10121075.
Kurzweil, F., Drost, K., Pašava, J., Wille, M., Taubald, H., Schoeckl, D., Schoenberg, R., 2015. Coupled sulfur, iron and molybdenum isotope data from black shales of the Teplá-Barrandian unit argue against deep ocean oxygenation during the Ediacaran. Geochimica et Cosmochimica Acta 171, 121–142.
Kuzmenkova, O.F., Shumlyanskyy, L.V., Nosova, A.A., Voskoboynikova, T.V., Grakovich, I.Y., 2011. Petrology and correlation of trap formations of the Vendian in the adjacent areas of Belarus and Ukraine. Lithosphere 35, 3–23.
Leblanc, M., Moussine-Pouchkine, A., 1994. Sedimentary and volcanic evolution of a Neoproterozoic continental margin (Bleida, Anti-Atlas, Morocco). Precambrian Research 70, 25–44.
Lerat, J.G., et al., 2018. Metals and radionuclides (MaR) in the Alum Shale of Denmark: Identification of MaR-bearing phases for the better management of hydraulic fracturing waters. Journal of Natural Gas Science and Engineering 53, 139–152.
Lenton, T.M., Boyle, R.A., Poulton, S.W., Shields-Zhou, G.A., Butterfield, N.J., 2014. Co-evolution of eukaryotes and ocean oxygenation in the Neoproterozoic era. Nature Geoscience 7, 257–265.
Letsch, D., Large, S.J.E., Buechi, M.W., Winkler, W., von Quadt, A., 2018. Ediacaran glaciations of the west African Craton – Evidence from Morocco. Precambrian Research 310, 17–38.
Li, Z.X., et al., 2008. Assembly, configuration, and break-up history of Rodinia: A synthesis. Precambrian Research 160, 179–210.
Macdonald, F.A. 2011. The Hula-Hula Diamictite and Katakturuk Dolomite, Arctic Alaska. In: Arnaud, E., Halverson, G.P. & Shields-Zhou, G. (eds) The Geological Record of Neoproterozoic Glaciations. Geological Society, London, Memoirs, 36, 379-387.
Mills, D.B., et al., 2014. Oxygen requirements of the earliest animals. Proceedings of the National Academy of Sciences 111, 4168–4172.
Mitchell, R.N., Gernon, T.M., Nordsvan, A., Cox, G.M., Li, Z., Hoffman, P.F., 2019. Hit or miss: Glacial incisions of snowball Earth. Terra Nova 31, 381–389.
Moore, E.K., Hao, J., Spielman, S.J., Yee, N., 2020. The evolving redox chemistry and bioavailability of vanadium in deep time. Geobiology 18, 127–138.
Mukherjee, I. & Large, R.R. 2020. Co-evolution of trace elements and life in Precambrian oceans: The pyrite edition. Geology, 48, 1018-1022.
Naidoo, D.D., Bloomer, S.H., Saquaque, A., Hefferan, K., 1991. Geochemistry and significance of metavolcanic rocks from the Bou Azzer-El Graara ophiolite (Morocco). Precambrian Research 53, 79–97.
New Energy Minerals 2019. Caula Graphite and Vanadium project. file:///C:/Users/gmi327/Desktop/Graphite-metal%20mixed%20exploration/NewEnergy%20Caula%20Graphite-VANADIUM%20Mozambique.html.
NextSource Materials 2017. The Green Giant Vanadium Project. https://www.nextsourcematerials.com/vanadium/green-giant-vanadium-project/.
Nosova, A.A., Kuz'menkova, O.F., Veretennikov, N.V., Petrova, L.G., Levsky, L.K., 2008. Neoproterozoic Volhynia-Brest Magmatic Province in the Western East European Craton: Within-plate magmatism in an ancient suture zone. Petrology 16 (2), 105–135.
Osanai, Y., Ueno, T., Tsuchiya, N., Takahashi, Y., Tainosho, Y., Shiraishi, K., 1990. Finding of vanadium-bearing garnet from the Sør Rondane Mountains, East Antarctica. Antarctic Record 34, 279–291.
Parasuraman, A., Lim, T.M., Menictas, C., Skyllas-Kazacos, M., 2013. Review of material research and development for vanadium redox flow battery applications. Electrochimica Acta 101, 27–40.
Parnell, J., Boyce, A.J., 2019. Neoproterozoic copper cycling, and the rise of metazoans. Scientific Reports 9, 3638.
Parnell, J., Brolly, C., Boyce, A.J., 2021. Graphite from Palaeoproterozoic enhanced carbon burial, and its metallogenic legacy. Geological Magazine 158 (9), 1711–1718.
Peng, H., 2019. A literature review on leaching and recovery of vanadium. Journal of Environmental Chemical Engineering 7, 103313.
Planavsky, N., Rouxel, O., Bekker, A., Lalonde, S.V., Konhauser, K.O., Reinhard, C.T., Lyons, T.W., 2010. The evolution of the marine phosphate reservoir. Nature 467, 1088–1090.
Sahoo, S.K., Planavsky, N.J., Kendall, B., Wang, X., Shi, X., Scott, C., Anbar, A.D., Lyons, T.W., Jiang, G., 2012. Ocean oxygenation in the wake of the Marinoan glaciation. Nature 489, 546–549.
Scherba, C., Montreuil, J.-F., Barrie, C.T., 2018. Geology and Economics of the Giant Molo Graphite Deposit, Southern Madagascar. Society of Economic Geologists Special Publication 21, 347–363.
Schlüter, J., Estrada, S., Lisker, F., Läufer, A., Kühn, R., Nitzsche, K.N., Spiegel, C., 2011. First petrographical description of rock occurrences in the Steingarden area, Dronning Maud Land, East Antarctica. Polarforschung 80, 161–172.
Schröder, S., Grotzinger, J.P., 2007. Evidence for anoxia at the Ediacaran-Cambrian boundary: the record of redox-sensitive trace elements and rare earth elements in Oman. Journal of the Geological Society, London 164, 175–187.
Shellnutt, J.G., Dostal, J., Keppie, J.D., 2004. Petrogenesis of the 723 Ma Coronation sills, Amundsen basin, Arctic Canada: implications for the break-up of Rodinia. Precambrian Research 129, 309–324.
Sperling, E.A., Carbone, C., Strauss, J.V., Johnston, D.T., Narbonne, G.M., Macdonald, F. A., 2016. Oxygen, facies, and secular controls on the appearance of Cryogenian and Ediacaran body and trace fossils in the Mackenzie Mountains of northwestern Canada. Geological Society of America Bulletin 128 (3-4), 558–575.
Środoń, J., Kuzmenkova, O., Stanek, J.J., Petit, S., Beaufort, D., Gilg, H.A., Liivamägi, S., Goryl, M., Marynowski, L., Szczerba, M., 2019. Hydrothermal alteration of the Ediacaran Volyn-Brest volcanics on the western margin of the East European Craton. Precambrian Research 325, 217–235.
Syrah Resources Ltd. 2021. Syrah Resources: Balama delivers up valuable vanadium by-product to complement graphite. https://www.proactiveinvestors.co.uk/companies/news/36572/syrah-resources-balama-delivers-up-valuable-vanadium-by-product-to-complement-graphite–43733.html.
Tellerreport 2019. Hard resistance to the mineral hunt: "There are no green mines". https://www.tellerreport.com/news/2019-11-12—hard-resistance-to-the-mineral-hunt–%22there-are-no-green-mines%22-.BJsKKvusr.html.
Wade, C.E., McAvaney, S.O., Gordon, G.A., 2014. The Beda Basalt: new geochemistry, isotopic data and its definition. MESA Journal 73, 24–41.
Wang, M., Huang, S., Chen, B., Wang, X., 2020. A review of processing technologies for vanadium extraction from stone coal. Mineral Processing and Extractive Metallurgy 129, 290–298.
Wang, X.-C., Li, X.-H., Li, Z.-X., Liu, Y., Yang, Y.-H., 2010. The Willouran basic province of South Australia: Its relation to the Guibei large igneous province in South China and the breakup of Rodinia. Lithos 119 (3-4), 569–584.
Williamson, N.M.B., Ootes, L., Rainbird, R.H., Bédard, J.H., Cousens, B., 2016. Initiation and early evolution of the Franklin magmatic event preserved in the 720 Ma Natkusiak Formation, Victoria Island. Canadian Arctic. Bulletin Volcanology 78, 19. https://doi.org/10.1007/s00445-016-1012-9.
Wu, T., Yang, R., Gao, L., Li, J., Gao, J., 2021. Origin and enrichment of vanadium in the Lower Cambrian Black Shales, South China. ACS Omega 6, 26870–26879.
Young, G.M., Gostin, V.A., 1989. An exceptionally thick upper Proterozoic (Sturtian) glacial succession in the Mount Painter area, South Australia. Geological Society of America Bulletin 101, 834–845.
Zhang, H., Lu, W., Li, X., 2019. Progress and Perspectives of Flow Battery Technologies. Electrochemical Energy Reviews 2, 492–506.
Zhang, Y.-M., Bao, S.-X., Liu, T., Chen, T.-J., Huang, J., 2011. The technology of extracting vanadium from stone coal in China: History, current status and future prospects. Hydrometallurgy 109 (1-2), 116–124.
Zhao, J., McCulloch, M.T., Korsch, R.J., 1994. Characterisation of a plume-related ~800 Ma magmatic event and its implications for basin formation in central-southern Australia. Earth and Planetary Science Letters 121, 349–367.
Zhuang, H., Lu, J., Fu, J., Liu, J., Ren, C., Zou, D., Tian, W., 1998. Organic/inorganic occurrence of metallic elements of the black shale-hosted Baiguoyuan silver-vanadium deposit in Xingshan, Hubei. Acta Geologica Sinica 72, 299–307.
Zi, J., Haines, P.W., Wang, X., Jourdan, F., Rasmussen, B., Halverson, G.P., Sheppard, S., Li, C., 2019. Pyroxene $^{40}Ar/^{39}Ar$ dating of basalt and applications to large igneous provinces and Precambrian stratigraphic correlations. Journal of Geophysical Research: Solid Earth 124, 8313–8330.